Coral Reefs
DOI 10.1007/s00338-014-1244-0

REPORT

Connectivity in the Intra-American Seas and implications for potential larval transport

H. Qian · Y. Li · R. He · D. B. Eggleston

Received: 28 March 2014 / Accepted: 4 November 2014

Abstract A major challenge in marine ecology is to describe patterns of larval dispersal and population connectivity, as well as their underlying processes. We re-assessed broad-scale population connectivity with a focus on the 18 coral reef hot spots in the Intra-American Seas described in Roberts (Science 278:1454–1457, 1997), by including seasonal and inter-annual variability in potential larval dispersal. While overall dispersal patterns were in agreement with previous findings, further statistical analyses show that dispersal patterns driven by mean circulation initially described by Roberts (Science 278:1454–1457, 1997) can significantly underestimate particle connectivity envelopes. The results from this study indicate that seasonal and inter-annual variability in circulation are crucial in modulating both dispersal distance and directional anisotropy of virtual larvae over most coral reef sites and that certain larval hotspots are likely more strongly connected than originally thought. Improved larval dispersal transport envelopes can enhance the accuracy of probability estimates which, in turn, may help to explain episodic larval settlement in certain times and places, and guide spatial management such as marine protected areas.

Keywords Intra-American Sea · Connectivity · Large-scale circulation

Communicated by Handling Editor Dr. Brian Helmuth

Electronic supplementary material The online version of this article (doi:10.1007/s00338-014-1244-0) contains supplementary material, which is available to authorized users.

H. Qian · Y. Li (✉) · R. He · D. B. Eggleston
Department of Marine, Earth, and Atmospheric Sciences, North Carolina State University, Raleigh, NC 27695, USA
e-mail: yli15@ncsu.edu

Introduction

A fundamental issue concerning recruitment dynamics of marine organisms and marine conservation biology involves identifying the paths of isolated populations connected by dispersal, and how spatiotemporal variation in the intensity of dispersal along these paths influences population connectivity, and the successful exchange of individuals among isolated populations (e.g., Cowen et al. 2007; Cowen and Sponaugle 2009; Young et al. 2012; Puckett et al. 2014). Most benthic marine organisms have limited mobility as adults such that dispersal, the transport and spread of larvae from natal origin during the pelagic larval stage, connects geographically isolated and demographically variable populations, forming a metapopulation (Levins 1969; Hanski 1998). There are four general challenges to improving our understanding of connectivity (Cowen and Sponaugle 2009; Edgar et al. 2014): (1) observations—determination of spatial scales of connectivity, (2) explanations—mechanisms underlying dispersal and connectivity, (3) consequences—impact of connectivity on population structure and dynamics, and (4) applications—issues of conservation and resource management. In this study, we applied an eddy-resolving ocean circulation and coupled particle-tracking model to assess the first two challenges: (1) the spatial scales of connectivity and (2) mechanisms underlying dispersal and connectivity. The patterns generated in this study will provide testable hypotheses in addressing the third and fourth challenges.

In a pioneer study by Roberts (1997), predicted mean ocean circulation and a corresponding particle-tracking model were used to map the routes of passive pelagic larvae originated from 18 different coral reef larval hotspots in the Caribbean Sea for dispersal durations of 1 and 2 months. The mapped connectivity patterns ("transport

Published online: 12 November 2014

envelopes") showed two general patterns of potential larval dispersal in the Caribbean: (1) upstream areas from which larvae could be imported, and (2) downstream areas to which larvae could be exported (Roberts 1997). Under conditions of mean ocean circulation, the 18 sites varied by an order of magnitude as either sources or recipients of larvae, with some sites showing high larval retention, while others showing relatively high contributions downstream, and others showing high dependence upon import from upstream sources. For example, Barbados is highly dependent upon local larval production and retention to replenish benthic populations and thus is risk-prone to recruitment overfishing, whereas the Bahamas and Florida Keys received the bulk of their larvae from upstream sources (see exceptions below) and were less risk-prone to recruitment overfishing. Since the publication by Roberts (1997), numerical modeling of ocean circulation and corresponding particle-tracking models have become more sophisticated, such as the integration of eddy-resolving ocean circulation and finer-scale resolution in the former, and integration of larval behavior and mortality in the latter (e.g., Cowen et al. 2000). Moreover, replenishment of benthic populations often relies on episodic recruitment events that correspond to daily, monthly and seasonal time scales (e.g., Sale et al. 1994; Eggleston et al. 1998, 2010; Doherty 2002) and may not be predicted under mean circulation patterns. The goal of this study was to compare and contrast relative dispersal envelopes under mean circulation (viz-a-viz Roberts 1997), with passive dispersal under seasonal and inter-annual time scales to determine whether spatiotemporal variation in circulation strongly alters patterns of larval connectivity in the Intra-American Seas.

The Intra-American Sea (IAS) is a semi-closed sea in the western Atlantic Ocean (Fig. 1). It is composed of the Caribbean Sea, the Gulf of Mexico (GOM), and the South Atlantic Bight (SAB). The circulation system in the IAS includes the Caribbean Current, which flows westward from the Lesser Antilles, passes through the Yucatan Channel as the Yucatan Current, then becomes the Loop Current in the GOM, and subsequently forms the Florida Current and Gulf Stream after it exits the GOM. The IAS circulation system is an integral part of the western boundary current in the North Atlantic Subtropical Gyre and of the meridional overturning circulation (Schmitz and Richardson 1991; Schmitz and McCartney 1993), and it plays an important role in transporting and dispersing water mass, heat, salt and other material. Understanding the transport connectivity within the IAS is therefore critical before any coupling with biology can be carefully undertaken.

Larval population connectivity has been a major research focus in the IAS since the 1990s, and this growing body of literature provides examples of broad-scale patterns of connectivity among sub-populations, as well as exceptions where local retention can be relatively important (e.g., Roberts 1997; Cowen et al. 2000, 2006; Lipcius et al. 2001; Paris and Cowen 2004; Young et al. 2012). For

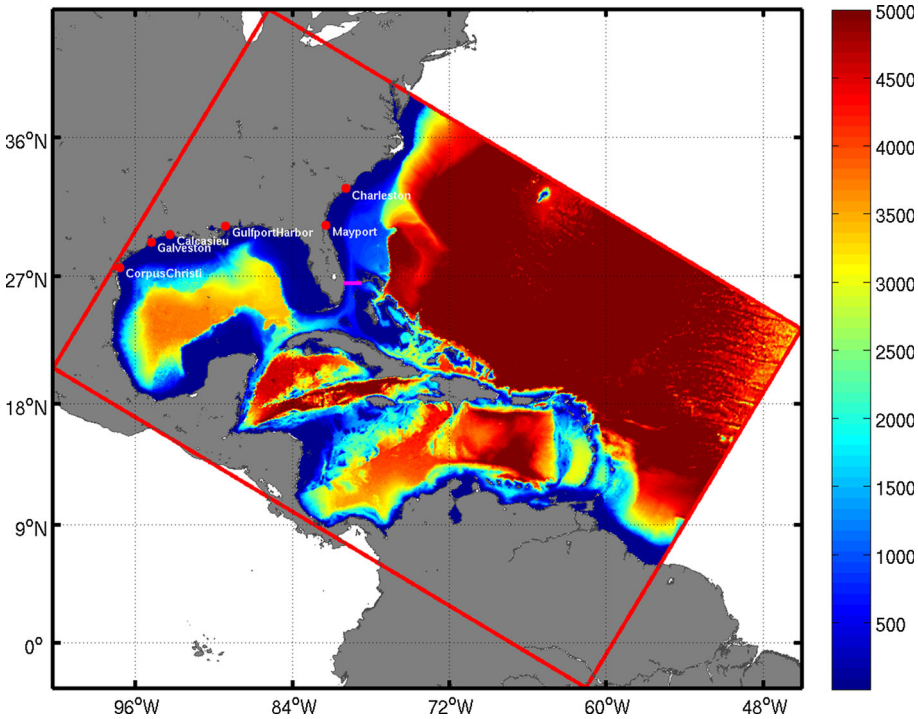

Fig. 1 Domain of 6-km resolution IAS circulation model overlaid with bathymetry in meters. *Red dots* represent locations of sea level stations from NOS. The *pink line* represents the transect location where the Florida Current transport is collected

example, although the Bahamas (not shown in this paper) and Florida Keys are predicted to receive the bulk of their larvae from numerous upstream sources (Roberts 1997; Cowen et al. 2006; Kough et al. 2013), certain water bodies and islands (keys) within the Bahamas and Florida can be strongly self-retentive at small spatial scales as a result of local gyre circulation (Lee and Williams 1999; Lipcius et al. 2001). Moreover, in deep-sea systems where current speeds can be an order of magnitude slower than surface currents, the general patterns of larval connectivity may be more restricted than those observed for surface-drifting larvae (Young et al. 2012).

Larval behavior and mortality can also modify patterns of larval dispersal and population connectivity (Jones et al. 1999; Cowen et al. 2000, 2006; Taylor and Hellberg 2003; Munday et al. 2009). For example, inclusion of a linear mortality function in a simple 2D circulation model greatly reduced dispersal envelopes for particles dispersing from Barbados compared to dispersal envelopes without larval mortality (Cowen et al. 2000). A related study applying a 3D, individual-based model that integrated biological parameters such as pelagic larval duration, vertical and horizontal swimming capabilities, and adult spawning strategies, determined that: (1) the Bahamas and the Turks and Caicos Islands exhibited high connectivity in the northern Caribbean and were largely isolated from the rest of the region; (2) the Nicaraguan archipelagos were strongly inter-connected; (3) the Panama-Colombia Gyre region was isolated from the rest of the Caribbean; and (4) the west and east Caribbean were moderately isolated from each other (Cowen et al. 2003). These studies provide an excellent foundation upon which to build for quantifying connectivity among different oceanic regions in the IAS. This study is unique in that: (1) the hydrodynamic and particle-tracking modeling approach is relatively sophisticated compared to previous simulations, and there were a large number of comparisons between predicted versus observed values to assess model performance, and (2) we consider seasonal and inter-annual variation in circulation and particle transport envelopes.

Methods

The general approach first involved quantifying the IAS circulation and particle transport connectivity at mean, seasonal and inter-annual time scales based on realistic, eddy-resolving circulation hindcast solutions during 2007–2010. Next, we quantified connectivity with a focus on the same 18 larval "hot spots" described in Roberts (1997), and then used statistically comprehensive Lagrangian probability density functions (LPDFs; Mitarai et al. 2009) to quantify the sources and destinations of virtual, passively drifting larvae.

Model setup

The IAS circulation model was constructed based on the Regional Ocean Modeling System (ROMS; Shcheptkin and McWilliams 2005; Haidvogel et al. 2008). ROMS is a free-surface, hydrostatic, primitive-equation model that employs split-explicit separation of fast barotropic and slow baroclinic modes and vertically stretched terrain-following coordinates. The IAS ROMS covers the entire Caribbean Sea, GOM and SAB, with a horizontal resolution of $\sim$6 km, sufficient for resolving mesoscale eddies in the IAS (Fig. 1). Vertically, there are 30 terrain-following levels, with increased resolution near the surface and bottom to better resolve boundary layer dynamics. The initial and open boundary conditions were provided by the global data assimilative Hybrid Coordinate Ocean Model (HYCOM). The global HYCOM assimilates satellite-observed sea surface temperature and height, and Argo measured temperature and salinity, providing daily circulation at about 10-km spatial resolution (http://hycom.rsmas.miami.edu/dataserver). At the land boundary, monthly mean discharge of 144 rivers in the IAS was imposed. The Mellor–Yamada closure scheme (Mellor and Yamada 1982) was applied to compute vertical turbulent mixing, as well as the quadratic drag formulation for the bottom friction specification.

Surface atmospheric forcing used to drive the IAS ROMS was obtained from the National Center for Environmental Prediction (NCEP) reanalysis (http://www.esrl.noaa.gov/psd/data/reanalysis/reanalysis.shtml), which has a spatial and temporal resolution of 1.875° and 6 h, respectively. Total cloud cover, precipitation, surface pressure, relative humidity, air temperature, surface wind, and net shortwave and long-wave radiations were used in the standard bulk formula (Fairall et al. 1996) to derive wind stress and net surface heat flux, which were used to drive the ocean circulation model. A one-yr simulation (January–December 2006) was used as the model spin-up, followed by a 4-yr simulation for the period from 2007 to 2010, the solutions of which were used for particle trajectory simulated described below.

Particle-tracking model and LPDFs

To study the connection among different oceanic domains and reef hotspots in the IAS, numerical surface particle trajectories were calculated using an offline particle-tracking model with a fourth-order Runge–Kutta tracking scheme, which has been widely used (Mitarai et al. 2009;

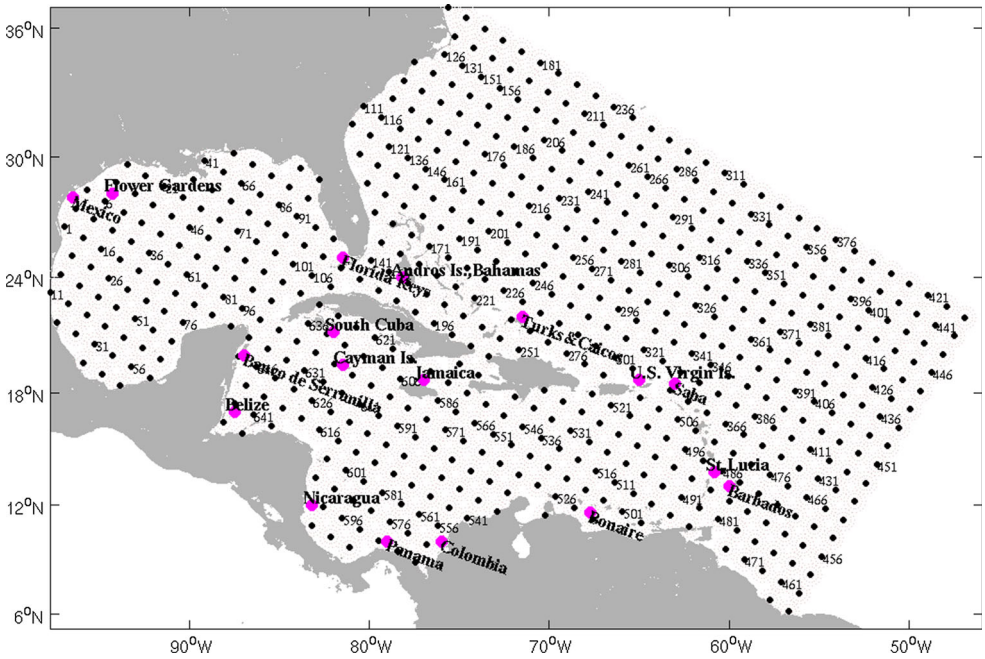

Fig. 2 Particle release locations. *Red dots* indicate the center of each release site, and *small black dots* represent particle release locations within a 60-km radius from release centers. *Pink dots* stand for the 18 coral reef hotspots (Andros Island, Bahamas, Florida Keys, Belize, Turks and Caicos Islands, Jamaica, Mexico, southern Cuba, Colombia, U.S. Virgin Islands, Bonaire, Saba, St. Lucia, Cayman Islands, Panama, Nicaragua, Flower Gardens, Barbados, and Banco de Serranilla) as in Roberts (1997)

Xue et al. 2009; Incze et al. 2010; Li et al. 2014). We selected a set of particle release centers that covered the IAS model domain at 120-km sampling intervals. Following the same approach of Mitarai et al. (2009), we chose each release site to be within a 60-km radius of the release center (Fig. 2). In this way, 650 release sites were defined that encompassed most regions in the IAS; however, in this study, we describe the results for the 18 coral reef "hotspots" modeled by Roberts (1997). At each site, a group of 45 particles was released every 10 d from 2007 to 2010 during the period of model simulation, and then tracked for up to 60 d. Thus, for each release site, there were 135 groups released (6,075 particles). This was sufficient for quantifying large-scale connectivity, as model sensitivity experiments using more particles (i.e., increased particle density) showed a similar dispersal pattern, a finding also documented by previous studies (e.g., Mitarai et al. 2009; Li et al. 2014).

The resulting particle trajectories were further quantified using Lagrangian probability density functions (LPDFs). Following Mitarai et al. (2009), we defined the LPDFs as the probability density of particle displacement. For a given set of advection time scales τ, sampling space variable ε, initial position $\mathbf{a}$, and the position of nth particle $X_n(\tau, a)$, the discrete representation of LPDFs $f'_X(\varepsilon; \tau, a)$ were defined as:

$$f'_X(\varepsilon;\tau,a) = \frac{1}{N}\sum_{n=1}^{N}\delta(X_n(\tau,a)-\varepsilon) \quad (1)$$

where N is the total number of Lagrangian particles, and δ is the Dirac delta function. The Dirac function is defined as the Heaviside function H in a unit area (i.e., $\delta = \frac{dH}{dxdy}$), where H is typically known as the unit step function, such that $H(x) = \begin{cases} 0 & \text{if } n < x \\ 1 & \text{if } n \geq x \end{cases}$, where n is the integer (grid number) along the x-axis. As such, f'_X is also in the unit of reciprocal area.

The discrete LPDF f'_X can be expressed as spatially averaged LPDFs over the surrounding area of each release site, that is:

$$f'_X(\varepsilon;\tau,a) \approx \frac{1}{\pi R^2}\int_{|r|\leq R} f'_X(\varepsilon;\tau,a+r)r\mathrm{d}r \quad (2)$$

where R is the radius of each release site (6 km in this study). A smooth operator (Gaussian filter with radius of 6 km) was then applied to remove sub-grid-scale noises to get the LPDF f_X. Compared to other conventional approach, the LPDF approach is a more rigid, statistically comprehensive way in quantifying the probability of particle traveling between source and destination locations (Mitarai et al. 2009; Li et al. 2014).

Model skill assessment

The model simulation provided eddy-resolving, spatial and temporal continuous circulation solutions. As an example, Fig. 3 presents a snapshot of the circulation field on June 1, 2010, in comparison with observed OSCAR near-surface current field (http://www.oscar.noaa.gov/). In the model, the Caribbean Current flowed westward from the Lesser Antilles with amplitude of ~ 1 m s^{-1}. It separated into two

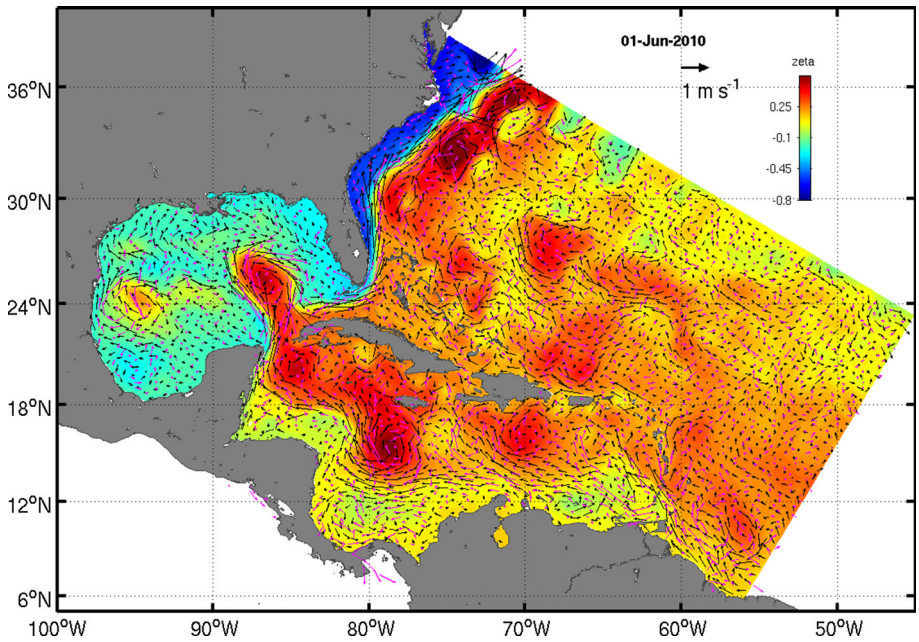

Fig. 3 A snapshot of sea surface height overlain with moded simulated (*black arrows*) and OSCAR surface velocity (*pink*) on June 1, 2010. A current vector scale of 1m s^{-1} is shown

flows near the Nicaraguan Rise, with the major current flowing north and westward toward the Yucatan Channel, and the smaller branch veering south to form the cyclonic Panama–Colombia Gyre (PCG). The major circulation features, including Yucatan Current and the Loop Current, as well as the Gulf Stream are all readily present and the flow very well aligns with the OSCAR current based on satellite observations (pink vectors in Fig. 3). The major circulation features, including Yucatan Current and the Loop Current, as well as the Gulf Stream are all readily present, and the modeled flow fields agree well with the satellite-based $0.25° \times 0.25°$ OSCAR (add reference) surface velocity maps (pink vectors in Fig. 3). The complex correlation (Li et al. 2009) between modeled and OSCAR currents is 0.82, further suggesting that model is capable of reproducing the general spatial structure of the currents.

To further evaluate the performance of the circulation model, we compared the model solutions with multiple satellite-based and in situ observations (Electronic Supplemental Material, ESM). A suite of observational data, including the (1) Florida Current (FC) Transport cable data, (2) AVISO (Archiving, Validation and Interpretation of Satellite Oceanographic Data) sea surface height anomaly, (3) sea level height, and (4) ship CTD casts were used to assess model performance. All these model validations suggest that the IAS ROMS can adequately resolve regional circulation and water mass properties, providing us confidence to carry out transport connectivity analyses.

Results

General particle trajectories in the IAS

The four-yr circulation model hindcast solutions drove the particle-tracking calculations, thereby allowing us to characterize particle transport and connectivity in the IAS. Particles released in the western GOM (e.g., Fig. 4a, release site 10) spread over northwest and central GOM. A small portion of particles traveled into the Gulf Stream, and dispersed as far as the SAB. Particles released in the central northern GOM (e.g., Fig. 4b, release site 39) dispersed both westward and eastward. The eastward moving particles reached the west Florida Shelf; some also entered the Florida Current and Gulf Stream and moved northward along the SAB. Particles released on the west Florida Shelf (e.g., Fig. 4c, release site 103) either remained in the local area or entered the Florida Current and the Gulf Stream, moving into the open ocean. Only a small portion of the particles moved northwestward to the central GOM. Particles released near Barbados (e.g., Fig. 4d, release site 482) generally demonstrated two major transport pathways. The first path entered the Caribbean Sea and moved northwestward, and the other path moved northwestward along the U.S. Virgin Islands and into the Sargasso Sea.

LPDFs and general coral reef connectivity

To illustrate the possible biological implications of circulation transport, we compared the upper bounds of the 18

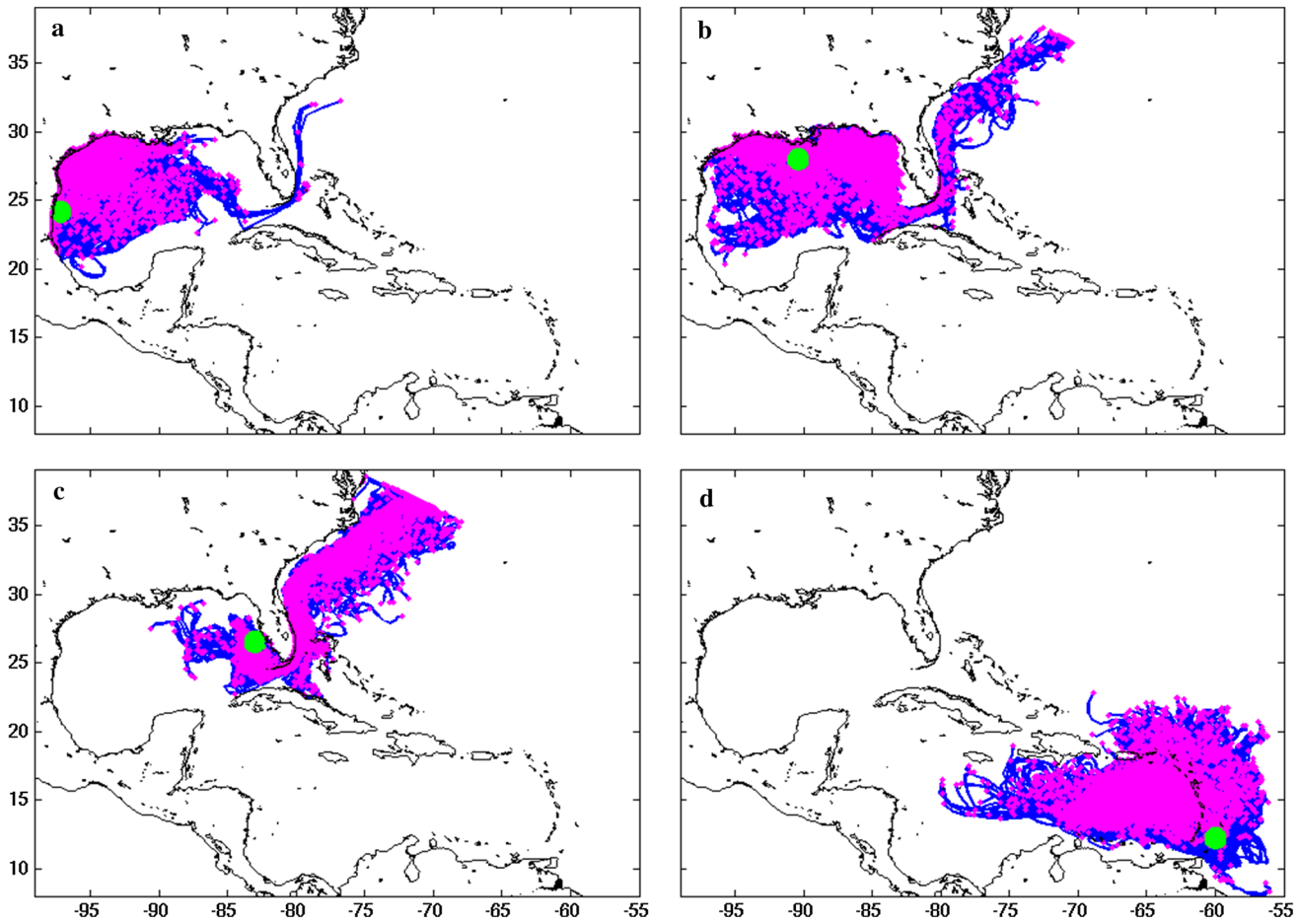

Fig. 4 Examples of particle trajectories with advection time of 60 d for four of the initial release locations as seen in Fig. 2. *Green dots* stand for starting points for the initial release locations, *blue line* stands for the particle trajectories, and *pink dots* represent the ending points (tails) of the initial release locations

coral reef "hot spot", transport envelopes defined by Roberts (1997) with the dispersal envelopes predicted from this study, which included seasonal and inter-annual variations in circulation (pink dots in Fig. 2). Because there is also potential for larvae to stay near its local habitat, the "upper bounds" herein indeed represent the highest likelihood of larval dispersal regardless of biological behavior (Roberts 1997). Lagrangian probability density functions (LPDFs) over the four-yr study period illustrate the probability of particles reaching certain destinations (Fig. 5). For example, particles released in the Cayman Islands had high probabilities of moving into the Loop Current after 60 d, as well as of being locally retained (Fig. 5a). Those particles might also have gone through the Florida Straits and continued northward to the SAB. Particles released at the Panama and Nicaragua sites had similar LPDF distributions (Fig. 5b, c), having high probabilities of staying in their local areas due to the presence of the permanent Panama–Colombia Gyre (PCG). Apart from remaining in the PCG area, particles released at Panama also exhibited a high probability of moving northwestward and entering the Loop Current after 60 d. Compared to the Panama release site, particles released at the Nicaragua site had smaller probabilities of moving northwestward and entering the GOM at the same advection time scale. Particles released at the Flower Gardens (Fig. 5d) showed high probabilities of dispersing both eastward and westward, though with limited travel distance. The LPDF distribution for particles released at Barbados (Fig. 5e) showed that particles had high probabilities moving into the Caribbean Sea, moving along the Virgin Islands, and staying in nearby regions after 60 d. In comparison with other release locations, particles released at Banco de Serranilla (Fig. 5f) showed a much more dispersive pattern. Particles had higher probabilities of leaving their local area, moving across the Yucatan Channel, reaching the south and central GOM, and being swept northward to the SAB.

Another way of illustrating particle dispersal patterns is in terms of mean dispersal distance (in kms) and angular direction in the Cartesian coordinate system (Fig. 6). Large

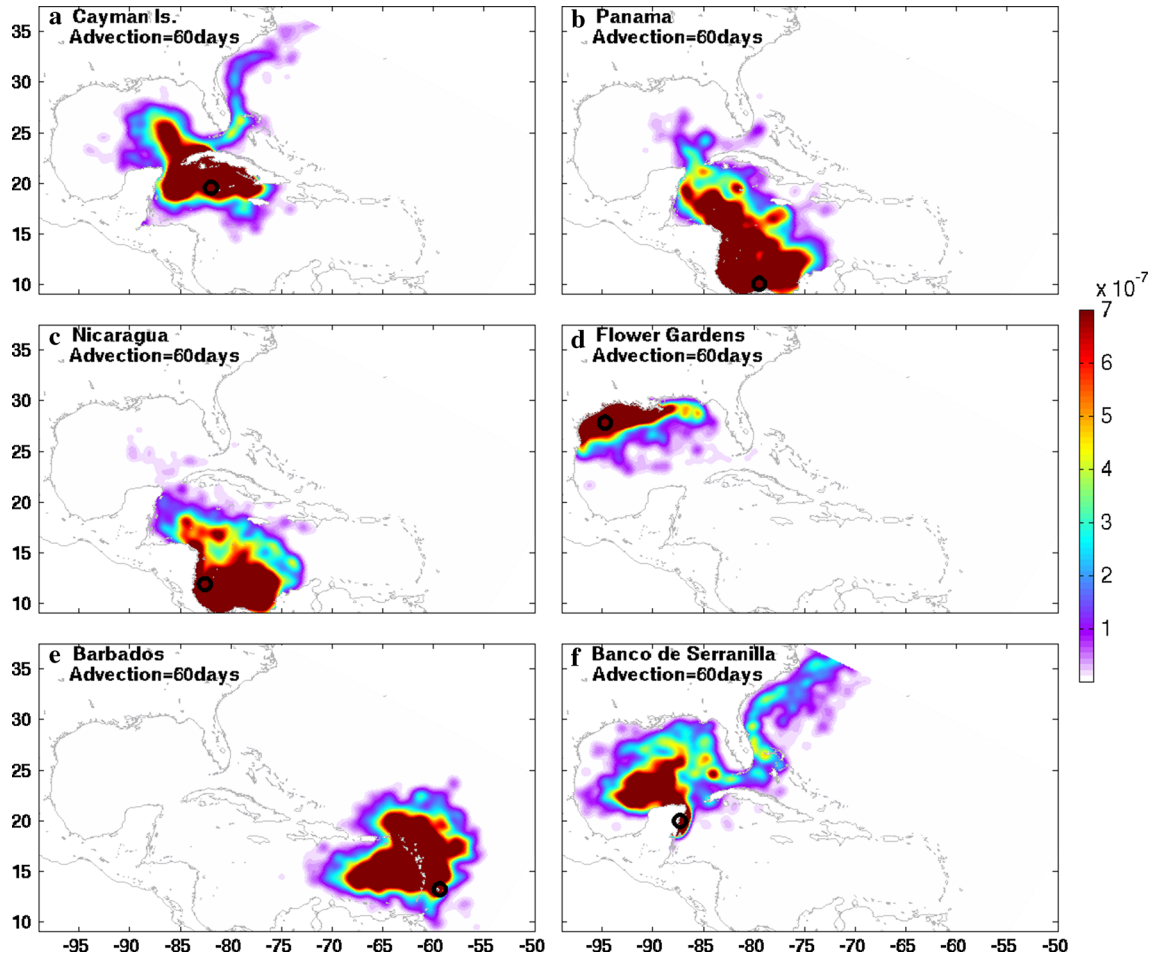

Fig. 5 Mean Lagrangian probability density functions (LPDFs in km^{-2}) for release sites from the Cayman Islands, Panama, Nicaragua, Flower Gardens, Barbados, and Banco de Serranilla with an advection time of 60 d. *Black dots* are release locations

variability exists among locations. For instance, in the western GOM region (Fig. 6a, b), the majority of particles (over 65 %) travelled 100–200 km with angles mainly at 0°, 110° and 180°, suggesting particles dispersed east- and northwestward. Particles in the Sargasso Sea region (Fig. 6c, d, e, f, g) generally dispersed over larger distances than the GOM. Over 50 % of the particles released from the Florida Keys travelled 1,700 km at a mean angle of 45° counterclockwise from the east. Particles released from Bahamas (Andros Island), dispersed mainly 100–300 km (over 50 %) or 1,600 km (over 12 %) at an angle of 90° east, showing the major northward movement of the particles. The distribution of dispersal distances for particles released from the Turks and Caicos Islands, U.S. Virgin Islands, and Saba demonstrated similar patterns, with the majority of the particles (~70 %) dispersing 300–700 km at 150° east, moving northwestward. Particles released from the northwest Caribbean region (Fig. 6h, i, j) showed limited travel distances. Approximately 60 % of the particles from those sites dispersed 100–300 km northwestward. Particles from Banco de Serranilla and Belize in the southwest Caribbean (Fig. 6k, l) demonstrated different dispersal patterns, with Banco de Serranilla showing a more dispersive pattern, while Belize exhibited a more retentive feature. At Banco de Serranilla (Fig. 6k), three peaks exist at 100, 500 and over 2,000 km. Particles released at Belize were mainly (~60 %) restricted to 100–200 km to the north. The dispersal distances for the particles in the Panama–Colombia region (Fig. 6m, n, o) become increasingly dispersive from Nicaragua to Panama to Colombia. At Colombia, 90 % of the particles dispersed relatively uniformly over a range of 100–1,400 km northwestward, with the highest percentage of particles traveling 700 km, and show a distinctive dispersive pattern. A majority of particles at Nicaragua (60 %) actually moved southward 100–300 km. This feature can be attributed to the cyclonic PCG at this region, which delivered particles from Nicaragua southward and moved the particles from Colombia northwestward. In the southeast Caribbean Sea (Fig. 6p), particles mainly moved

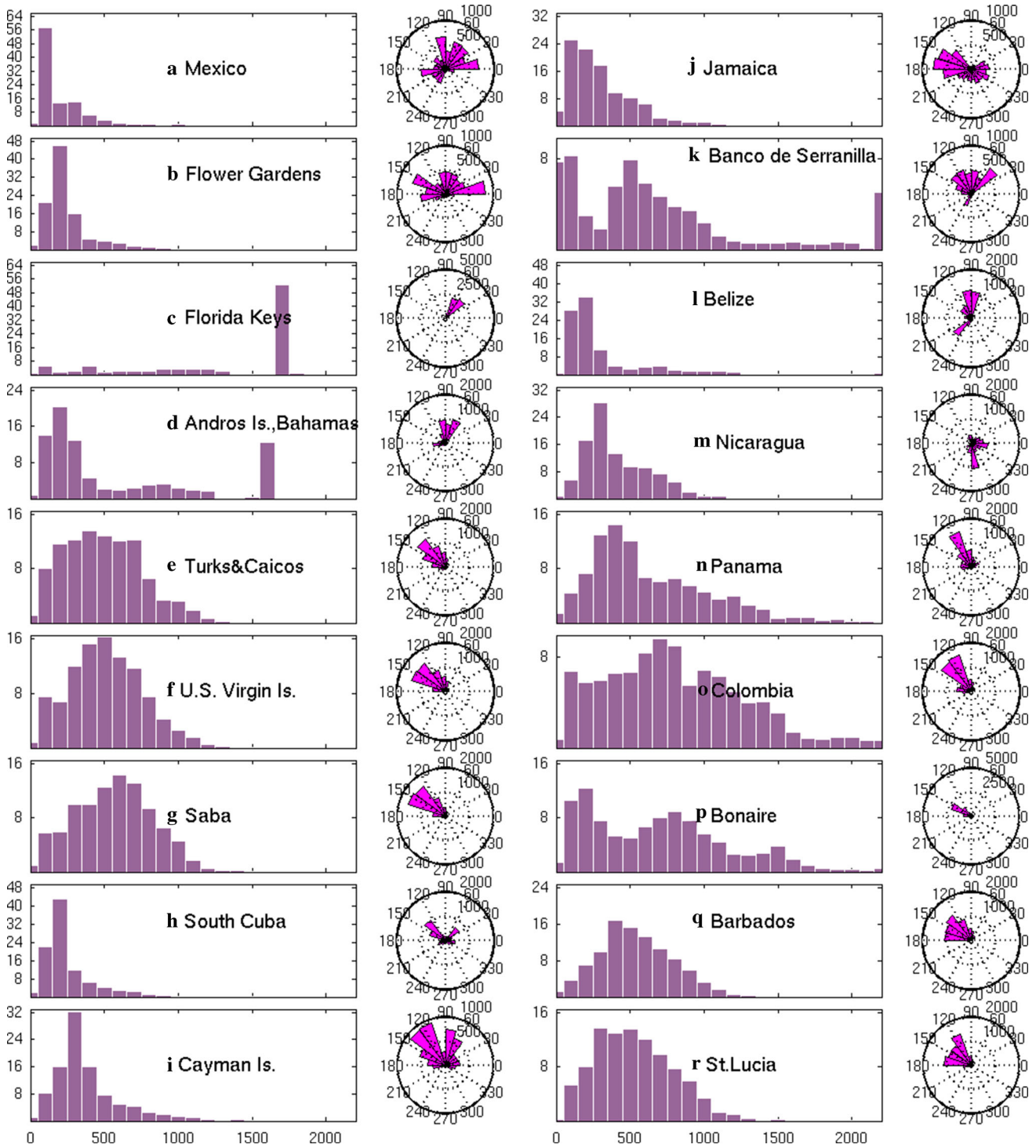

Fig. 6 Dispersal distance and angular histograms for particles released from 18 coral reef sites from 2007 to 2010 with an advection time of 60 d. *x*-axis unit is km, and *y*-axis is percentage

northwestward at many distances. In the Antilles region (Fig. 6q, r), around 60 % of the particles moves in the northwestward direction 300–700 km.

It is clear that dispersal distance and directions are different for the 18 coral reef hotspots as a result of ocean circulation. Overall, our results suggest that regions like Florida Keys and southwestern Caribbean region shows more dispersive patterns, while regions in the western GOM and southeastern Caribbean Sea are more self-retentive and solely reply on local supply for

Table 1 *P* values (*df*) from one-way analysis of variance (ANOVA) tests of whether or not mean dispersal distance (first two columns) or angular trajectories (last two columns) vary according year for 18 coral reef sites: AI (Andros Islands, Bahamas), FK (Florida Keys), BE (Belize), TC (Turks and Caicos), JA (Jamaica), ME (Mexico), SC (southern Cuba), CO (Colombia), UVI (U.S. Virgin Island), BO (Bonaire), SA (Saba), SL (St. Lucia), CI (Cayman Island), PA (Panama), NI (Nicaragua), FG (Flower Gardens), BA (Barbados), and BS (Banco de Serranilla)

Stations	ANOVA test (*p*) for dispersal distance	ANOVA test (*p*) for angular trajectory of particles
AI	0*	0.0001*
FK	0.0075*	0.0001*
BE	0*	0*
TC	0*	0.0003*
JA	0.9730	0*
ME	0.0401*	0*
SC	0.0129*	0.1524
CO	0*	0.0195*
UVI	0*	0*
BO	0.0148*	0*
SA	0*	0*
SL	0*	0*
CI	0.0003*	0*
PA	0.0004*	0.2542
NI	0*	0*
FG	0*	0*
BA	0*	0*
BS	0.0524	0.0027*

* Statistically significant differences among years ($\alpha = 0.05$). Sample size is 650 to test the difference between 4 yr. Advection time is 60 d

Table 2 Same of Table 1, but for the ANOVA test of seasonal variations of dispersal distance and angular trajectory of particles

Stations	ANOVA test (*p*) for dispersal distance	ANOVA test (*p*) for angular trajectory of particles
AI	0*	0*
FK	0*	0*
BE	0*	0*
TC	0*	0*
JA	0*	0*
ME	0*	0*
SC	0.0136*	0*
CO	0*	0*
UVI	0.0017*	0.1771
BO	0.0008*	0*
SA	0.4306	0*
SL	0.0001*	0*
CI	0*	0*
PA	0*	0*
NI	0*	0*
FG	0.0010*	0*
BA	0*	0*
BS	0.5208	0.0884

replenishment. This essentially supports Roberts' results (Roberts 1997) that is based on a mean circulation pattern to drive the larval dispersions.

Seasonal and inter-annual variability of coral reef connectivity

In addition to mean particle dispersal, the seasonal and inter-annual variability of transport connectivity was also investigated for the 18 coral reef sites. Sixteen out of 18 coral reefs sites showed significant differences in dispersal distance and angular trajectory among years and seasons (Tables 1, 2, respectively). For illustration purposes, we chose two release sites (Florida Keys and Andros Island, Bahamas) to describe their inter-annual (Fig. 7a) and seasonal (Fig. 7b) variability in connectivity patterns. We noted some difference in dispersal from year to year (Fig. 7a). For example, the dispersal distance in 2009 and 2010 from Andros Island, Bahamas was more self-retentive compared to previous years. In 2009 and 2010, 70 % of the particles traveled within 400 km distance from their release site, which is substantially higher percentage compared to about 48 % in 2007 and 2008. Further, only 10 % (9 %) of the particles dispersed over 1,600 km in 2009 (2010), while in 2007 and 2008, over 20 % of the particles traveled over 1,600 km. The overall dispersal pattern changed from bimodal in 2007 and 2008 to more like a single peak in 2009 and 2010. The inter-annual variation in distribution in the angular direction is also noticeable in these years for particles released at Bahamas Islands. In 2009 and 2010, though a majority of the particles were still moving northward, more particles were moving westward than in 2007 and 2008. At the Florida Keys site, 50 % of the particles in 2007 moved over 1,500 km with the Gulf Stream with a single peak distribution, however, in other years, the dispersal distribution was bimodal with peaks at both 1,700 and 1,800 km from their nature source.

The seasonal variability of particle dispersal was also apparent for most of the coral reef sites (Fig. 7b, more statistics later). For instance, the dispersal distances of the majority of particles released at Andros Island, Bahamas in winter were 200–300 km, compared to other seasons when particles traveled over 1,500 km. In addition, the amount of particles moving westward in winter was comparable to that moving northward, whereas only a small portion of particles moved westward in other seasons as a result of seasonal variations in the circulation during 2007–2010. Thus, inter-annual and seasonal variability are important factors in modulating particle dispersal at most of the coral reef sites

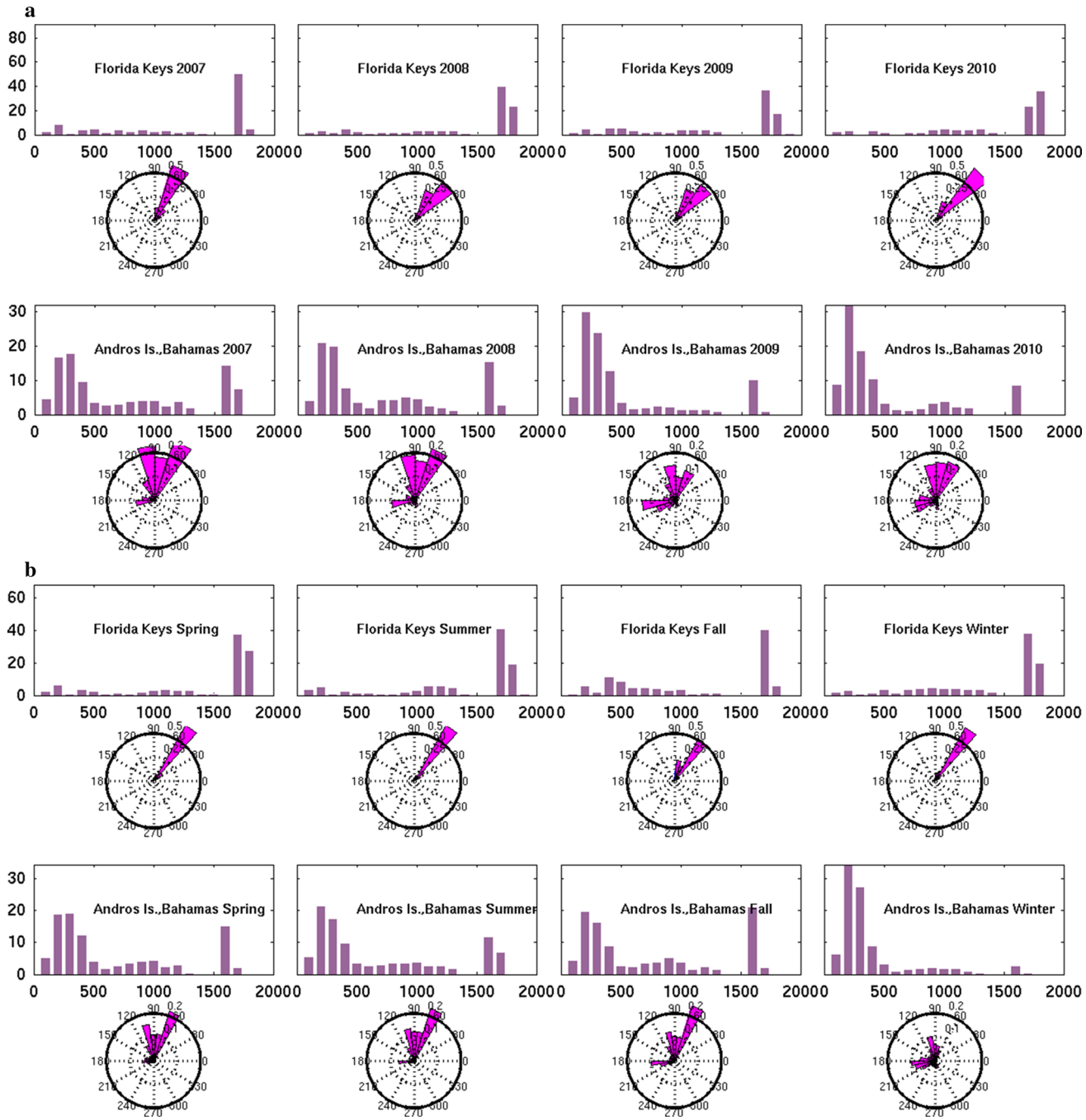

Fig. 7 **a** Examples of inter-annual variability in dispersal distance and angular directional histograms for particle release sites at the Florida Keys, USA, and Bahamas (Andros Island) from 2007 to 2010 with an advection time of 60 d. **b** Examples of seasonal variability in dispersal distance and angular directional histograms for the Florida Keys and the Bahamas. y-axes are in the units of kms

examined in the IAS, and therefore must be carefully taken into consideration when estimating dispersal potential.

Comparison of particle dispersal envelopes with Roberts (1997)

The importance of seasonal and inter-annual variability is also reflected in the mean export envelops (Fig. 8). We calculated the particle export envelops after advection of 30 and 60 d for six representative coral reef locations. There were similarities in the basic envelop shapes between our analyses and the results of Roberts (1997). While the large-scale pattern is similar between our model and Roberts (1997), one major discrepancy is that for all six locations, the export envelops computed in our analyses cover much larger areas than those of Roberts (1997). All

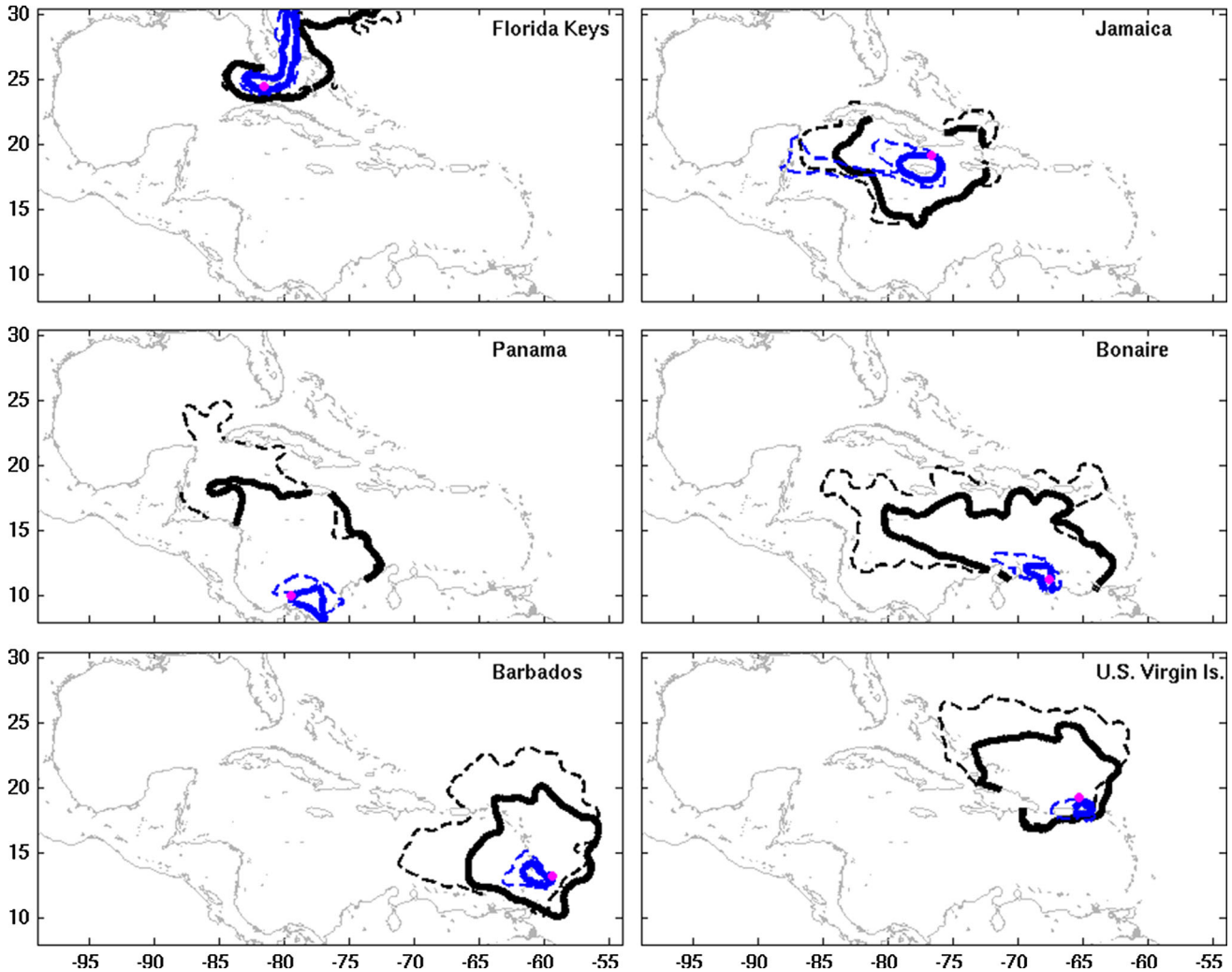

Fig. 8 Mean particle export envelopes defined by the LPDFs for six coral reef locations (Florida Keys, Jamaica, Panama, Bonaire, Barbados, and U.S. Virgin Islands). In each panel, both 30-d (*solid lines*) and 60-d (*dashed lines*) envelopes are shown, with model-simulated envelopes in *black* and the envelopes adapted from Roberts (1997) in *blue*. *Pink dots* represent initial release locations

the envelopes computed in this study is essentially >60 % larger than Roberts (1997) in terms of occupied area of larval dispersal for both 30- and 60-d advection time scales. For certain region, such as Panamas site, the envelope is up to five times the area of previous defined. What may have led to a larger envelope? Our study took into consideration the high-frequency (synoptic, seasonal and inter-annual) variability associated with surface currents, while Roberts (1997) used only mean surface currents. Indeed, the model-simulated mean surface currents and their corresponding variance ellipses (Fig. 9) indicated that the variability of surface currents was significant in most regions of IAS. The current variational ellipses were larger compared to their mean flow in western GOM, northwest Caribbean Sea near Cuba, northeast Caribbean Sea and deep seas. Particle dispersals from these areas therefore experience more variations apart from the mean. In contrast, in regions such as the major flow system of the Caribbean Current, Loop Current and Gulf Stream, the mean flow overwhelms the major variations in general. Current variability is not negligible and can modulate the particle trajectory. Therefore, relying solely on the mean surface currents to track passive particles may be suitable to obtain general patterns, but may be biased in resolving details and variability in transport envelope quantification. This is also one of the factors that lead to the fact that marine protected areas (MPAs) often failed to reach their full potential (Edgar et al. 2014).

Discussion

This study used an ocean circulation and coupled particle-tracking model to address two challenges to improving our

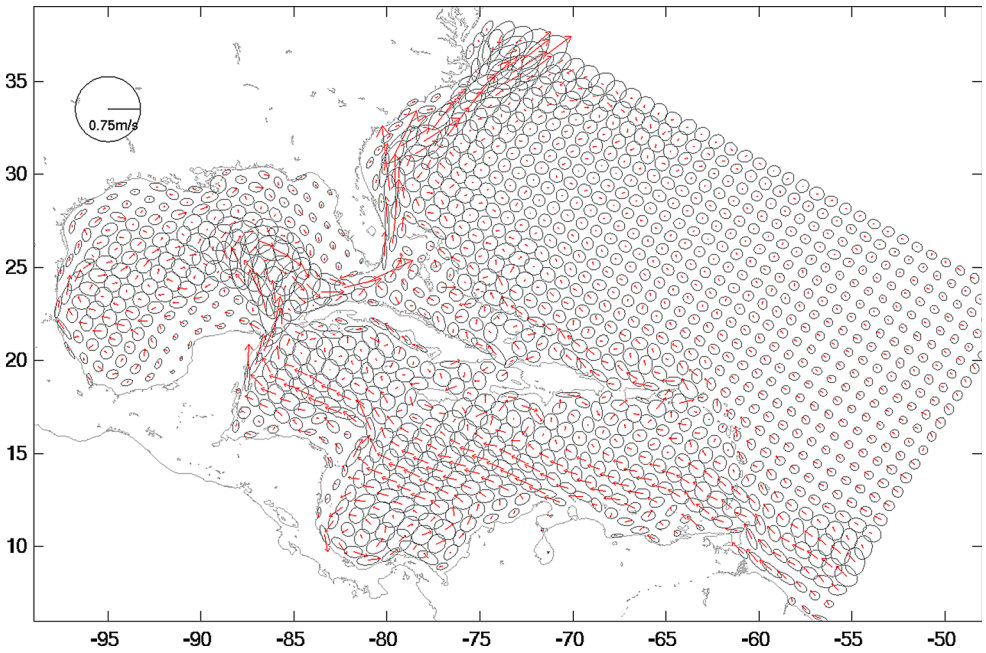

Fig. 9 Mean surface circulation (*red vectors*) and current variance ellipses (*black ovals*) for the IAS. A vector scale of 0.75 m s^{-1} is shown

understanding of population connectivity in marine systems: (1) spatial scales of connectivity and (2) mechanisms underlying dispersal and connectivity (Edgar et al. 2014). In this study, dispersal distance and direction under mean circulation varied among the 18 coral reef hotspots in a manner similar to the study by Roberts (1997), with larvae released from regions such as the Florida Keys and southwestern Caribbean region dispersing larvae broadly downstream, whereas larvae released from regions in the western GOM and southeastern Caribbean Sea being more self-retentive, such that the latter regions likely rely more on local supply for population replenishment than upstream sources. Conversely, inclusion of seasonal and inter-annual variation in circulation and corresponding larval dispersal in this study increased variation in the direction that larvae dispersed and increased the spread of particles approximately fivefold compared to dispersal under average conditions. The increase in variability of dispersal direction and spread of particles suggests that the spatial scale of population connectivity in the IAS is much greater than originally thought (e.g., particles dispersed 1,000–2,000 km). These results support empirical observations by ecologists of episodic settlement by reef fish larvae in certain places and times (Danilowicz 1997). These episodic settlement events can deliver a cohort of a given species to a specific reef or region, sometimes delivering a large year-class that can drive population dynamics (Caley et al. 1996). The increased spatial scales of potential larval dispersal, combined with episodic delivery of larvae driven by inter-annual and seasonal variation in circulation patterns identified in this study, likely facilitate metapopulation persistence over time (Sale 2002).

Model performance

The predicted values from the ocean circulation model hindcast and particle-tracking computer simulations during 2007–2010 were consistent with observations of circulation, eddy kinetic energy, surface dynamic topography, coastal sea level variation, as well as vertical distributions of temperature and salinity. This model–data comparisons provided herein are essential, as the model skill assessment is not yet extensively examined and exhibited for the IAS region (e.g., Roberts 1997; Sheng and Tang 2004; Sheng 2006), but are indeed the fundamental basis for any follow-up analysis.

Potential larval dispersal

Mean particle dispersal in this study varied among sites due to different circulation dynamics. For example, particles released from the southwestern Caribbean and Florida Keys moved downstream and were either entrained into the GOM loop current (SW Caribbean), or covered a large area of the SAB and Gulf Stream (FL Keys or SW Caribbean). Larval entrainment into the Gulf Stream from these spawning regions is consistent with a recent bio-physical study of larval dispersal of Caribbean spiny lobster (*Panulirus argus*), which suggested that the strong flows associated with the Caribbean current and eventually Gulf Stream serve as a type of "graveyard" for larval lobsters

because high mean flows wash larvae into the North Atlantic where few will survive (Kough et al. 2013).

There were other similarities between the results of this study and those of Kough et al. (2013), even though we simulated pelagic larval durations (PLDs) of 1 and 2 months, whereas Kough et al. (2013) simulated pelagic larval durations of ~6 months. For example, both studies suggested that there is relatively strong local retention of larvae when spawned in the northwest Caribbean and Bahamas, which could serve as a "larval nursery" (Kough et al. 2013). Kough et al. (2013) indicated that pelagic larval nurseries occurred offshore of Nicaragua, southwestern Cuba and the central Bahamas, and suggested, based on dispersal simulations with and without larval behavior, that larval nursery zones were governed by oceanographic features and not larval behavior.

Examination of current variation ellipses in this study provide evidence to support the idea of certain regions serving as either larval "graveyards" or "nurseries." For example, current variation ellipses were larger compared to their mean flow in western GOM, northwest Caribbean Sea near Cuba, northeast Caribbean Sea and deep seas. Particle dispersal from these areas therefore experiences more variation apart from the mean. In contrast, in regions such as the major flow system of the Caribbean Current, Loop Current and Gulf Stream, the mean flow overwhelms local variation in circulation.

This study and that by Kough et al. (2013) also suggested areas such as Honduras, Puerto Rico and the Florida Keys depend on upstream sources of larvae and that the southeast Caribbean depends primarily on local retention to support pelagic larval recruitment. One specific example is that particles released from the Antilles region remained primarily near their natal sources, with some particles moving westward into the Caribbean Sea or northwestward along the island chain. Kough et al. (2013) indicated that the Columbia and Panama regions were strongly dependent upon upstream sources of larvae, whereas our study suggested that these regions had relatively high local retention. These differences may have been due to the relatively short PLD of larvae in our study (1 to 2 months) versus a relatively long PLD in the study by Kough et al. (2013), which may have allowed larvae of long PLD to eventually "leak" out of the gyre circulation that promoted local retention.

In addition to the mean dispersal patterns discussed above, significant inter-annual and seasonal variability in particle dispersal envelopes was demonstrated for 16 of the 18 coral reef sites in our study. Our results also showed that the upper limit in quantifying fish larval transport (i.e., most distant point that a particle may reach) defined by Roberts (1997) was under-estimated nearly fivefold, supporting the conclusion that higher-frequency variation in circulation patterns should be integrated into numerical models to improve the accuracy of predicted larval dispersal envelopes (e.g., Putman and He 2013).

Our transport and connectivity analyses only considered ocean physics. The transport envelopes generated are therefore the upper bounds of possible transport envelopes for coral reef species (Jones et al. 1999). Species-oriented studies considering biological behaviors (i.e., swimming, growth, mortality, etc.), such as Cowen et al. (2000, 2006) and Kough et al. (2013), and their coupling with ocean circulation are needed to better assist coastal management and design of marine protected areas across state and country borders. In addition, timing of the spawning can vary depending on species and geographic locations. Therefore, our 4-yr mean envelopes may not be representative of dispersal patterns for seasonal-spawning larvae. A weighting of the LPDFs between peak and off-peak seasons may be needed to better represent these envelopes. Based on in situ magnetically attractive particles (MAPs), Hrycik et al. (2013) showed that the dispersal kernel e-folding scale is sensitive to the diffusivity coefficient. Due to lack of in situ observations, we could not estimate diffusion in our case; rather a harmonic horizontal viscosity coefficient of 100 m^2 s^{-1} is used, following Marchesiello et al. (2003).

We recognize that predictions of larval connectivity from our modeling results are somewhat limited in terms of resolving small-scale oceanographic features that may be important to dispersal, retention and recruitment of coral and fish larvae. For example, although larvae spawned from nearshore coral reefs are generally advected offshore, they may concentrate along the shelf-break (Marancik et al. 2012) or in nearby gyres and meanders (Porch 1998), and subsequently rely on periodic oceanic (frontal eddies: Sponaugle et al. 2005) and wind events (Eggleston et al. 1998) to move onshore toward settlement and nursery habitats. Growing evidence suggests that auditory and olfactory cues are also important mechanisms enabling larvae to orient and, in some cases for relatively strong-swimming larvae, swim toward settlement habitat (Simpson et al. 2008; Vermeij et al. 2010; Wolanksi and Kingsford 2014). We suggest that the results of our study provide a broad spatial-scale perspective on potential larval connectivity among sub-populations and that further research is needed to determine the relative importance of small-scale oceanographic features, such as frontal zones and eddies, in potentially modifying patterns of larval connectivity identified in this study.

Nevertheless, this study provides valuable insight in how circulation at seasonal and inter-annual timescales may change larval dispersal potential and is vital in any future bio-physical simulations of particle dispersal (i.e., phytoplankton, zooplanktons, nutrients and pollutants). Improved larval dispersal transport envelopes provide more

accurate probability estimates that, in turn, may help to explain episodic larval settlement in certain times and places, and guide spatial management such as marine protected areas.

Acknowledgments We thank Dr. Daniel Kamykowski for providing constructive comments that help to improve the quality of the manuscript. We are grateful to CNES France and ERA for providing AVISO SSH data, and NOAA AMOL and NOS for providing Florida current transport and coastal sea level data available online. This work was part of Dr. Hui Qian's Ph.D. dissertation under the supervision of Dr. Ruoying He at North Carolina State University. Research support was provided by NSF OCE 1029841.

References

Caley MJ, Carr MH, Hixon MA, Hughes TP, Jones GP, Menge BA (1996) Recruitment and the local dynamics of open marine populations. Annu Rev Ecol Syst 27:477–500

Cowen RK, Sponaugle S (2009) Larval dispersal and marine population connectivity. Annu Rev Mar Sci 1:443–466

Cowen RK, Paris CB, Srinivasan A (2006) Scaling of connectivity in marine populations. Science 311:522–527

Cowen RK, Paris CB, Olson DB, Fortuna JL (2003) The role of long distance dispersal in replenishing marine populations. Gulf Caribb Res 14:129–137

Cowen RK, Lwiza KM, Sponaugle S, Paris CB, Olson DB (2000) Connectivity of marine populations: open or closed? Science 287:857–859

Cowen RK, Gawarkiewicz GG, Pineda J, Thorrold SR, Werner FE (2007) Population connectivity in marine systems: an overview. Oceanography 20:14–21

Danilowicz BS (1997) A potential mechanism for episodic recruitment of a coral reef fish. Ecology 78:1415–1423

Doherty PJ (2002) Variable replenishment and the dynamics of reef fish populations. In: Sale PF (ed) Coral reef fishes: dynamics and diversity in a complex ecosystem. Academic Press, San Diego, CA, pp 327–355

Edgar GJ, Stuart-Smith RD, Willis TJ, Kininmonth S, Baker SC, Banks S, Barrett NS, Becerro MA, Bernard ATF, Berkhout J, Buxton CD, Campbell SJ, Cooper AT, Davey M, Edgar SC, Försterra G, Galván DE, Irigoyen AJ, Kushner DJ, Moura R, Parnell PE, Shears NT, Soler G, Strain EMA, Thompson RJ (2014) Global conservation outcomes depend on marine protected areas with five key features. Nature 506:216–220

Eggleston DB, Lipcius RN, Marshall LS, Ratchford SG (1998) Spatiotemporal variation in postlarval recruitment of the Caribbean spiny lobster in the central Bahamas: lunar and seasonal periodicity, spatial coherence, and wind forcing. Mar Ecol Prog Ser 174:33–49

Eggleston DB, Reyns NB, Etherington LL, Plaia G, Xie L (2010) Tropical storm and environmental forcing on regional blue crab settlement. Fish Oceanogr 19:89–106

Fairall CW, Bradley EF, Rogers DP, Edson JB, Young GS (1996) Bulk parameterization of air-sea fluxes for tropical ocean-global atmosphere Coupled-Ocean Atmosphere Response Experiment. J Geophys Res 101:3747–3764

Haidvogel DB, Arango H, Budgell P, Cornuelle BD, Curchitser E, Di Lorenzo E, Fennel K, Geyer W, Hermann A, Lanerolle L, Levin J, McWilliams JC, Miller AJ, Moore AM, Powell TM, Shchepetkin AF, Sherwood CR, Signell RP, Warner JC, Wilkin J (2008) Ocean forecasting in terrain-following coordinates: Formulation and skill assessment of the Regional Ocean Modeling System. J Comput Phys 227:3595–3624

Hanski I (1998) Metapopulation dynamics. Nature 396:41–49

Hrycik JM, Chassé J, Ruddick BR, Taggart CT (2013) Dispersal kernel estimation: A comparison of empirical and modelled particle dispersion in a coastal marine system. Estuar Coast Shelf Sci 133:11–22

Incze L, Xue H, Wolff N, Xu D, Wilson C, Steneck R, Wahle R, Lawton P, Pettigrew N, Chen Y (2010) Connectivity of lobster (*Homarus americanus*) populations in the coastal Gulf of Maine: part II- Coupled biophysical dynamics. Fish Oceanogr 19:1–20

Jones GP, Milicich MJ, Emslie MJ, Lunow C (1999) Self-recruitment in a coral reef fish population. Nature 402:802–804

Kough AS, Paris CB, Butler MJ (2013) Larval connectivity and the international management of fisheries. PLoS ONE 8:e64970

Lee TN, Williams E (1999) Mean distribution and seasonal variability of coastal currents and temperature in the Florida Keys with implications for larval recruitment. Bull Mar Sci 64:35–56

Levins R (1969) Some demographic and genetic consequences of environmental heterogeneity for biological control. Bull Entomol Soc Am 15:237–240

Li Y, He R, Manning JP (2014) Coastal connectivity in the Gulf of Maine in spring and summer of 2004–2009. Deep-Sea Res II 103:199–209

Li Y, He R, McGillicuddy DJ, Anderson DM, Keafer BA (2009) Investigation of 2006 *Alexandrium fundyense* bloom in the Gulf of Maine: In situ observations and numerical modeling. Cont Shelf Res 29:2069–2082

Lipcius RN, Stockhausen WT, Eggleston DB (2001) Marine reserves for Caribbean spiny lobster: empirical evaluation and theoretical metapopulation recruitment dynamics. Mar Freshw Res 52:1589–1598

Marancik KE, RichardsonDE Lyczkowski-Shultz J, Cowen RK, Konieczna K (2012) Spatial and temporal distribution of grouper larvae (Serranidae: Epinephelinae: Epinephelini) in the Gulf of Mexico and Straits of Florida. Fish Bull 110:1–20

Marchesiello P, McWilliams JC, Shchepetkin A (2003) Equilibrium structure and dynamics of the California Current System. J Phys Oceanogr 33:753–783

Mellor LG, Yamada T (1982) Development of a turbulence closure model for geophysical fluid problems. Rev Geophys 20:851–875

Mitarai SD, Siegel A, Watson JR, Dong C, McWilliams JC (2009) Quantifying connectivity in the coastal ocean with application to the Southern California Bight. J Geophys Res 114:C10026

Munday PL, Leis JM, Lough JM, Paris CB, Kingsford MJ, Berumen ML, Lambrechts J (2009) Climate change and coral reef connectivity. Coral Reefs 28:379–395

Paris CB, Cowen RK (2004) Direct evidence of a biophysical retention mechanism for coral reef fish larvae. Limnol Oceanogr 49:1964–1979

Porch CE (1998) A numerical study of larval fish retention along the southeast Florida coast. Ecol Model 109:35–59

Puckett BJ, Eggleston DB, Kerr PC, Luettich R (2014) Larval dispersal and population connectivity among a network of marine reserves. Fish Oceanogr 23:342–361

Putman NF, He R (2013) Tracking the long-distance dispersal of marine organisms: Sensitivity of ocean model resolutions. J R Soc Interface 10:20120979

Roberts CM (1997) Connectivity and management of Caribbean coral reefs. Science 278:1454–1457

Sale PF (2002) Coral reef fishes: Dynamics and diversity in a complex ecosystem. Academic Press, New York, p 527

Sale PF, Guy GA, Steel WJ (1994) Ecological structure of assemblages of coral reef fishes on isolated patch reefs. Oecologia 98:83–99

Schmitz WJ, Richardson PL (1991) On the sources of the Florida Current. Deep- Sea Res Suppl. 32:S379–S409

Schmitz WJ, McCartney MS (1993) On the North Atlantic circulation. Rev Geophys 31:29–49

Shcheptkin AF, McWilliams MC (2005) A split-explicit, free-surface, topographic following-coordinate oceanic model. Ocean Model 9:347–404

Sheng J (2006) Circulation and variability over the Meso-American Barrier Reef System: Application of a triply nested ocean circulation model. Estuarine and Coastal Modeling 9:270–290

Sheng J, Tang L (2004) A two-way nested-grid ocean-circulation model for the Meso-American Barrier Reef System. Ocean Dynamics 54:232–242

Simpson SD, Meekan MG, Jeffs A, Montgomery JC, McCauley RD (2008) Settlement-stage coral reef fish prefer the higher-frequency invertebrate-generated audible component of reef noise. Anim Behav 75:1861–1868

Sponaugle S, Lee T, Kourafalou V, Pinkard D (2005) Florida Current frontal eddies and the settlement of coral reef fishes. Limnol Oceanogr 50:1033–1048

Taylor MS, Hellberg ME (2003) Genetic evidence for local retention of pelagic larvae in a Caribbean reef fish. Science 299:107–109

Vermeij MJA, Marhaver KL, Huijbers CM, Nagelkerken I, Simpson SD (2010) Coral larvae move toward reef sounds. PLoS ONE 5:e10660

Wolanksi E, Kingsford MJ (2014) Oceanographic and behavioural assumptions in models of the fate of coral and coral reef fish larvae. J R Soc Interface 11:20140209

Xue H, Incze L, Xu D, Wolff N, Pettigrew N (2009) Connectivity of lobster populations in the coastal Gulf of Maine, Part I: Circulation and larval transport potential. Ecol Model 210:193–211

Young C, He R, Emlet R, Li Y, Qian H, Arellano S, Van Gaest A, Bennett K, Wolf M, Smart T, Rice M (2012) Dispersal of deep-sea larvae from the Intra-American Seas: Simulations of trajectories using ocean models. Integr Comp Biol 52:483–496